ROBUST CONTROL OF LOW-COST DIRECT DRIVES BASED ON INTERIOR PERMANENT MAGNET SYNCHRONOUS MOTORS

S.M. Peresada[*], D.I. Rodkin[**], Y.O. Nikonenko[***], S.M. Kovbasa[****], V.V. Polischuk
National Technical University of Ukraine "Igor Sikorsky Kyiv Polytechnic Institute",
Peremohy Ave., 37, Kyiv, 03056, Ukraine, e-mail: **sergei.peresada@gmail.com.**

Torque ripple compensation problem is considered for electrical drives, based on low-cost direct drive interior permanent magnet synchronous motors. Robustness properties of the speed and position control systems have been studied using time scale separation properties of the current, speed and position control loops. It is shown that system closed-loop dynamics according to new controller design has cascaded properties with speed and position control loops connected in series and therefore has potential of high frequency torque ripple compensation by increasing controllers gains. Experimental results are presented for two motors with similar rated data but significantly different level of the torque ripple. It is shown that despite of significand difference in parasitic torque amplitude, the similar position control performance can be achieved. It makes proposed control algorithms suitable for both high dynamic performance and low-cost direct drive applications with medium performance requirements. References 13, figures 7.
Keywords: interior permanent magnet synchronous motors, robust speed control, position control, torque ripple.

Introduction. Interior permanent magnet synchronous motors (IPMSMs) are widely used in high performance applications due to superior efficiency, power and torque density. One of the biggest disadvantages of the PMSMs is presence of parasitic torque pulsations which lead to control performance degradation, especially at low speeds. The problem of torque ripple compensation is not a new one. It was intensively studied in 1990s and early 2000s. Today this problem is becoming even more relevant due to increasing popularity of small electric vehicles and emergence of numerous low-cost direct IPMSM drives. Term low-cost in this case refers to IPMSMs with simplified rotor and stator structures, and that are built from cheap lower quality materials.

Major sources of the resulting torque ripple are caused by deviations from a sinusoidal flux density distribution around the airgap, by deficiencies of feasible winding geometries, and by the variable magnetic reluctance of the airgap due to the stator slots [1]. One of the approaches to reduce pulsating torque is to modify motor design [2, 3]. Several methods aiming to reduce the cogging torque in PMSMs, such as rotor skewing, modification of permanent magnets pole arc width, notches in the stator teeth and shifting of the permanent magnets are compared in [2]. Influence of rotor skewing on torque ripple depending on magnets design is examined in [3].

Another approach is to compensate or suppress the torque ripple using special control algorithms [1], [4–8]. Deadbeat current controller with compensation of flux and cogging harmonics is proposed in [1], [4]. In [5] reduction of torque ripple caused by flux harmonics is achieved by usage of high bandwidth current loop repetitive controller in parallel with linear proportional-integral controller (PI controller). The iterative learning control module and torque estimation module are designed and used in parallel with PI current and speed controllers to minimize torque pulsations in [6]. Adaptive control algorithm is presented in [7]. Adaptive law for estimation of the amplitudes of high order flux harmonics is designed using the second Lyapunov method. Similar approach is presented in [8]. In the paper, it is assumed that frequencies of torque oscillations are known. In [9] modified iterative learning control scheme implemented in frequency domain is proposed. Genetic algorithms that find optimal current pair to reduce torque ripple are presented in [10].

Application of the adaptive control technique requires development of the torque ripple model, whose characteristic pattern of produced harmonic torque may be different even when compared to identical machines from the same producer and the same production batch. As a result, self-commissioning is required for each individual machine, which is impractical for low-cost applications.

The one possible option in this case would be to use a basic control algorithm which is sufficiently robust to uncompensated perturbations that cause torque pulsations. In [11, 12] authors proposed a new cas-

ORCID ID: [*] https://orcid.org/0000-0001-8948-722X; [**] https://orcid.org/0000-0002-9235-2999;
[***] https://orcid.org/0000-0003-2379-5566; [****] https://orcid.org/0000-0002-2954-455X

caded structure for speed and position control systems, which is robust to parametric and dynamic uncertainties such as friction and time-varying load torque.

The aim of this work is to verify and prove by simulation and experimentally that speed and position feedback linearizing control algorithms for IPMSMs [11, 12] are robust to uncompensated perturbations including torque oscillations and can be used in low-cost drives.

Model of IPMSM. The model of the IPMSM in rotor reference frame (d-q) is the following

$$
\begin{aligned}
\dot{\theta} &= \omega, \\
\dot{\omega} &= J^{-1}\left[1.5p_n\left((L_d - L_q)i_d i_q + \psi_m i_q\right) - \nu\omega - T_L - T_P\right], \\
\dot{i}_d &= L_d^{-1}(-Ri_d + L_q p_n \omega i_q + u_d), \\
\dot{i}_q &= L_q^{-1}(-Ri_q - L_d p_n \omega i_d - \psi_m p_n \omega i_d + u_q),
\end{aligned}
\tag{1}
$$

where θ is rotor angular position; ω is the rotor speed; u_d, u_q and i_d, i_q are stator voltages and currents respectively; ψ_m is the permanent magnets flux; T_L is the load torque; R is the stator windings active resistance; L_d, L_q are (d-q) stator inductances; ν is the viscous friction coefficient; J is the total inertia; p_n is number of pole pairs; T_P is the rapidly varying parasitic torque.

Feedback linearizing position tracking control algorithm. The algorithm has been designed based on concepts, given in [11], for $i_d^* = 0$. Block-diagram of the position tracking control algorithm is shown in Fig. 1. Controller guarantees asymptotic position tracking if position reference θ^* is smooth and bounded function with bounded first $\dot{\theta}^*$, second $\ddot{\theta}^*$ and third $\dddot{\theta}^*$ time derivatives.
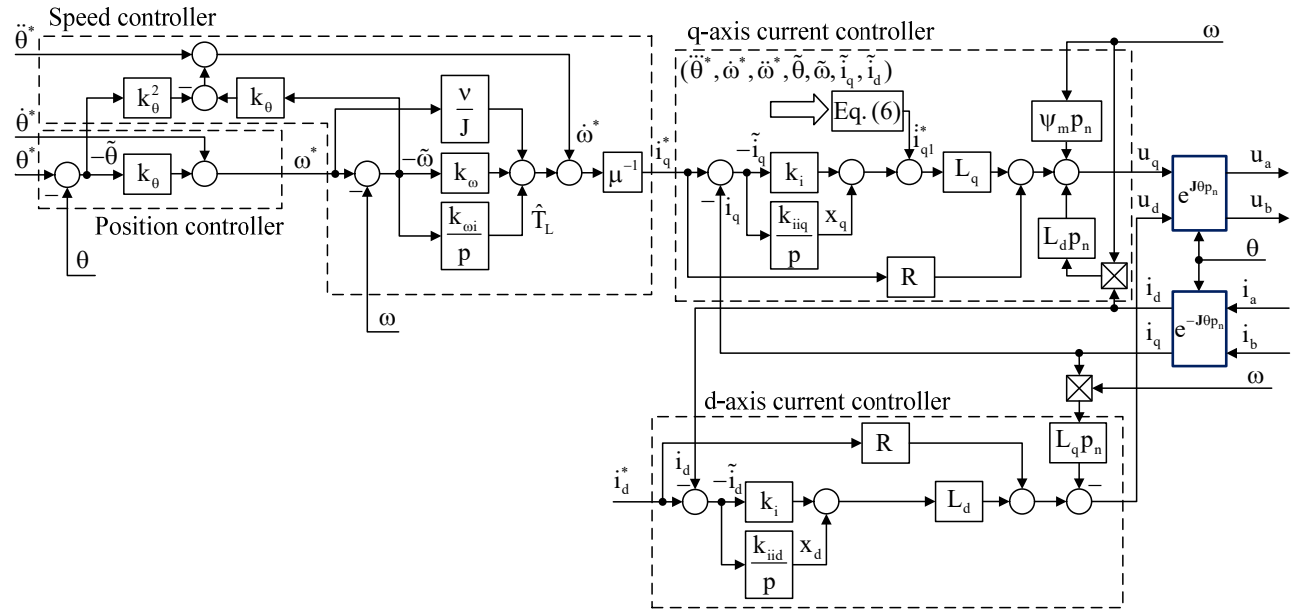
Fig. 1

Position controller has the following form:

$$
\omega^* = -k_\theta \tilde{\theta} + \dot{\theta}^*,
\tag{2}
$$

where $k_\theta > 0$ is position controller proportional gain; $\tilde{\theta} = \theta - \theta^*$ is the position tracking error; ω^* is the speed reference.

Speed controller equations are given by

$$
\begin{aligned}
i_q^* &= \frac{1}{\mu}\left(\frac{\nu}{J}\omega^* + \dot{\omega}^* + \hat{T}_L - k_\omega \tilde{\omega}\right), \\
\dot{\hat{T}}_L &= -k_{\omega i}\tilde{\omega},
\end{aligned}
\tag{3}
$$

where $\tilde{\omega} = \omega - \omega^*$ is the speed tracking error; i_q^* is a quadrature current reference; $\mu = 3p_n\psi_m / 2J$; $(k_\omega, k_{\omega i}) > 0$ is the speed controller proportional and integral gains; $\hat{T}_L$ is the estimate of the slowly varying

load torque component T_L / J; $\tilde{T}_L = (T_L / J) - \hat{T}_L$ is the estimation error of T_L / J; the first time derivative of the speed reference (2) is computed as

$$\dot{\omega}^* = -k_\theta \left(-k_\theta \tilde{\theta} + \tilde{\omega} \right) + \ddot{\theta}^*. \tag{4}$$

Current controllers are defined as

$$u_q = Ri_q^* + L_d p_n \omega i_d + \psi_m p_n \omega i_d + L_q \left(-k_i \tilde{i}_q + x_q + i_{q1}^* \right), \quad u_d = Ri_d^* - L_q p_n \omega i_q + L_d \left(-k_i \tilde{i}_d + x_d \right),$$
$$\dot{x}_q = -k_{iiq} \tilde{i}_q, \qquad\qquad\qquad\qquad\qquad\qquad \dot{x}_d = -k_{iid} \tilde{i}_d, \tag{5}$$

where $k_i > 0$ is the current controllers proportional gain; $\tilde{i}_q = i_q - i_q^*$ is the quadrature current tracking error; $k_{iid}, k_{iiq} > 0$ is the current controllers integral gains along d and q axes respectively; known component of the time derivative of quadrature current reference is the following:

$$i_{q1}^* = \frac{1}{\mu} \left(\frac{\nu}{J} \dot{\omega}^* + \ddot{\omega}^* + \dot{\hat{T}}_L \right) - \frac{k_\omega}{\mu} \left(-\left(\frac{\nu}{J} + k_\omega \right) \tilde{\omega} + \mu \tilde{i}_q + \frac{3}{2J} p_n \left(\left(L_d - L_q \right) \tilde{i}_d i_q \right) \right), \tag{6}$$

where $\tilde{i}_d = i_d - i_d^*$, the second derivative of the speed reference (2) is given by

$$\ddot{\omega}^* = -k_\theta \left(-k_\theta \left(-k_\theta \tilde{\theta} + \tilde{\omega} \right) - \left(\frac{\nu}{J} + k_\omega \right) \tilde{\omega} + \mu \tilde{i}_q + \frac{3}{2J} p_n \left(\left(L_d - L_q \right) \tilde{i}_d i_q \right) \right) + \dddot{\theta}^*. \tag{7}$$

The equations of the resulting closed-loop error dynamics of the position control system are:

$$\dot{\tilde{\theta}} = -k_\theta \tilde{\theta} + \tilde{\omega}, \tag{8}$$

$$\dot{\tilde{\omega}} = -k_{\omega 1} \tilde{\omega} - \tilde{T}_L - \frac{T_P}{J} + \mu \tilde{i}_q + \frac{3}{2J} p_n \left(\left(L_d - L_q \right) \tilde{i}_d \left(\tilde{i}_q + i_q^* \right) \right), \tag{9}$$

$$\dot{\tilde{T}}_L = k_{\omega i} \tilde{\omega}, $$

$$\dot{\tilde{i}}_q = -k_{iq} \tilde{i}_q + x_q - \frac{k_\omega + k_\theta}{\mu} \left(\tilde{T}_L + \frac{T_P}{J} \right), \tag{10}$$

$$\dot{x}_q = -k_{iiq} \tilde{i}_q, $$

$$\dot{\tilde{i}}_d = -k_{id} \tilde{i}_d + x_d, $$

$$\dot{x}_d = -k_{iid} \tilde{i}_d, \tag{11}$$

where $k_{\omega 1} = k_\omega + \nu / J$, $k_{iq} = k_i + R / L_q$, $k_{id} = k_i + R / L_d$.

Error dynamics analysis. The direct current error dynamics (11) is asymptotically stable $\forall (k_{i1}, k_{ii}) > 0$ and decoupled from (8) – (10), i.e. $\lim_{t \to \infty} (\tilde{i}_d, x_d) = \mathbf{0}$. Therefore the system dynamics (8) – (10) can be considered with $\tilde{i}_d = 0$.

System (8) – (10) is stable with suitable tuning of controllers gains. According to theory of cascaded systems, the quadrature current dynamics (10) has to be at least two times faster than the speed loop dynamics (9). At the same time the speed dynamics has to be faster than the position dynamics.

Another approach of current control loop tuning is high-gain tuning. In this case the following analysis can be applied.

Quadrature current dynamics (10) analysis is provided considering transformation $\eta = \varepsilon^{-1} \tilde{i}_q$, where $\varepsilon = k_{iq}^{-1}$. Dynamics (10) in new coordinates becomes

$$\dot{\eta} = -k_{iq} \eta - \frac{\tilde{x}_q}{\varepsilon},$$
$$\dot{\tilde{x}}_q = \lambda k_{iq} \eta + \frac{k_\omega + k_\theta}{\mu} \left(\dot{\tilde{T}}_L + \frac{\dot{T}_P}{J} \right), \tag{12}$$

where $\tilde{x}_q = \mu^{-1} (k_\omega + k_\theta)(\tilde{T}_L + T_P / J) - x_q$, $\lambda = 0.25$ if damping factor $\xi = 1$, $\lambda = 0.5$ if $\xi = \sqrt{2} / 2$.

System (12) can be rewritten as

$$\varepsilon\dot\eta = -\eta - \tilde{x}_q,$$
$$\varepsilon\dot{\tilde{x}}_q = \lambda\eta + \varepsilon\frac{k_\omega + k_\theta}{\mu}\left(\dot{\tilde{T}}_L + \frac{\dot{T}_P}{J}\right). \tag{13}$$

For small enough $\varepsilon < 1$, closed-loop system (8) – (11) will be a singularly perturbed one. Therefore, if k_{iq} is high enough, the reduced-order solution condition $\lim_{t\to\infty}\tilde{i}_q = 0$ can be achieved with $\varepsilon = 0$. Worth mentioning that the increase of k_ω and k_θ gains lead to increased influence of parasitic component T_P / J and torque estimation error $\tilde{T}_L$ on quadrature current dynamics.

Considering that with suitable tuning, condition $\lim_{t\to\infty}(\tilde{i}_q, \tilde{i}_d) = \mathbf{0}$ is fulfilled, the speed and position dynamics (9), (10) can be simplified to

$$\dot{\tilde{\theta}} = -k_\theta\tilde{\theta} + \tilde{\omega},$$
$$\dot{\tilde{\omega}} = -k_{\omega 1}\tilde{\omega} - \tilde{T}_L - \frac{T_P}{J}, \tag{14}$$
$$\dot{\tilde{T}}_L = k_{\omega i}\tilde{\omega}.$$

Analysis of (14) shows that the speed dynamics, given by the last two equations of (14), and the position dynamics are connected in series. It means that speed error $\tilde{\omega}$ caused by the presence of uncompensated parasitic torque appears in position dynamics as an external disturbance. Therefore, its influence on position error can be decreased by increase of the position gain k_θ.

Speed tracking algorithm. Speed tracking algorithm equations are presented in (3), (5) and (6) with speed reference ω^* and its derivatives $\dot\omega^*, \ddot\omega^*$ given as external functions of time.

Resulting closed-loop dynamics in this case is presented in (9) – (11) with $k_\theta = 0$ and therefore the same error dynamics analysis can be applied.

Simulation and experimental results. The experiments are carried out using the rapid prototyping station, whose functional diagram is shown in Fig. 2. Station includes: tested PMSMs; three-phase MOSFET-based SVPWM-controlled inverter operated at 15 kHz switching frequency; DSP TMS320F28335 based controller, which performs data acquisition, implements control algorithms with programmable tracing of selected variables; personal computer for processing, programming, interactive oscilloscope, data acquisition, etc. The motor speed is meas-
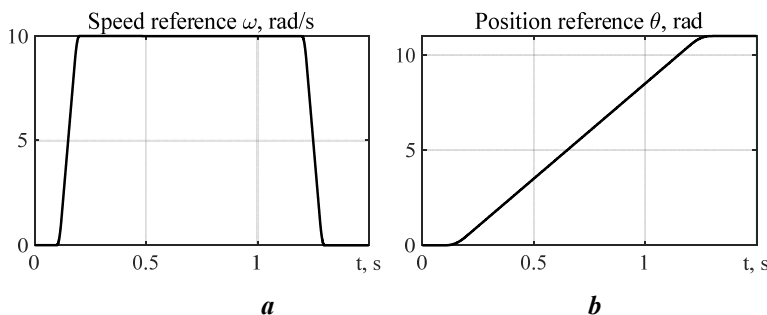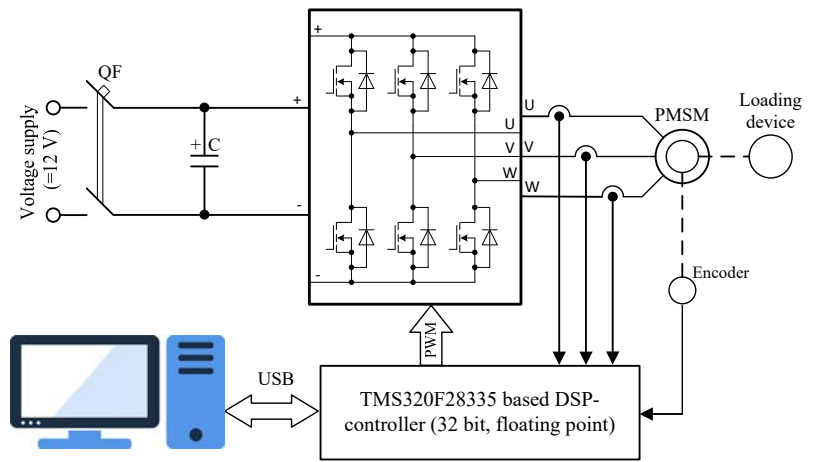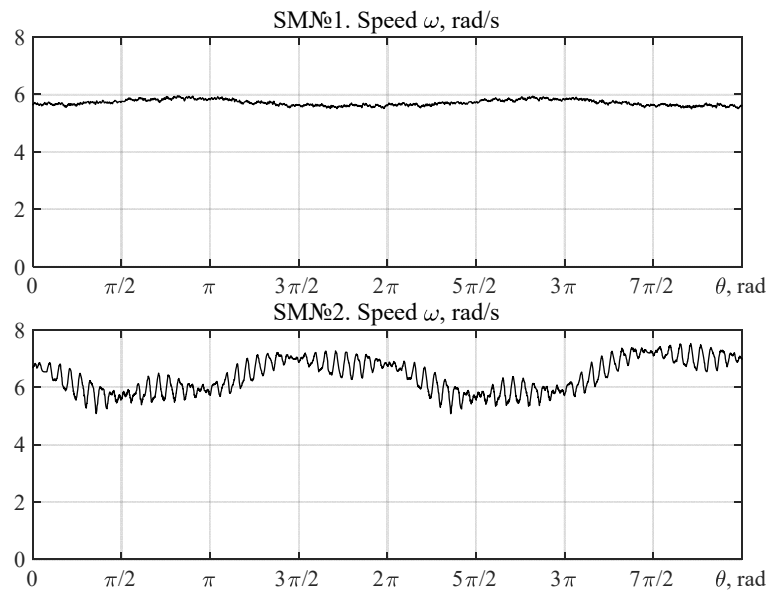
Fig. 2

SM№1. Speed ω, rad/s

SM№2. Speed ω, rad/s

Fig. 3

Speed reference ω, rad/s

Position reference θ, rad

a

b

Fig. 4

ured by a 4096 pulse/revolution optical encoder. The sampling time is set at 150 μs.

Robust position tracking controller has been tested by simulation and experimentally using two different motors SM1 and SM2, having different levels and content of torque ripple, as it follows from the speed wave-forms of the rotor free rotation, shown on Fig. 3. Motor rated data are listed in the Appendix A. The results of electrical parameters identification for both motors are presented in the Appendix B.

Speed trajectory tracking. The operation sequence, shown in Fig. 4, a has been applied. Motor starts the acceleration stage at t = 0.1 s from the zero speed to 10 rad/s and decelerates at t = 1.2 s. Acceleration and deceleration time is 0.1 s. Maximum values of the first and the second speed reference derivatives are $\dot{\omega}^* = 125$ rad/s^2, $\ddot{\omega}^* = 6250$ rad/s^3 respectively. Controller gains are tuned at: $k_\omega = 200$, $k_{\omega i} = k_\omega^2 / 2$, $k_{i1} = 1000$, $k_{iid} = (k_{i1} + R/L_d)^2 / 4$, $k_{iiq} = (k_{i1} + R/L_q)^2 / 4$. Transients of speed trajectory tracking are presented in Fig. 5.

a - SM1 simulation	b - SM1 experiment	c - SM2 experiment
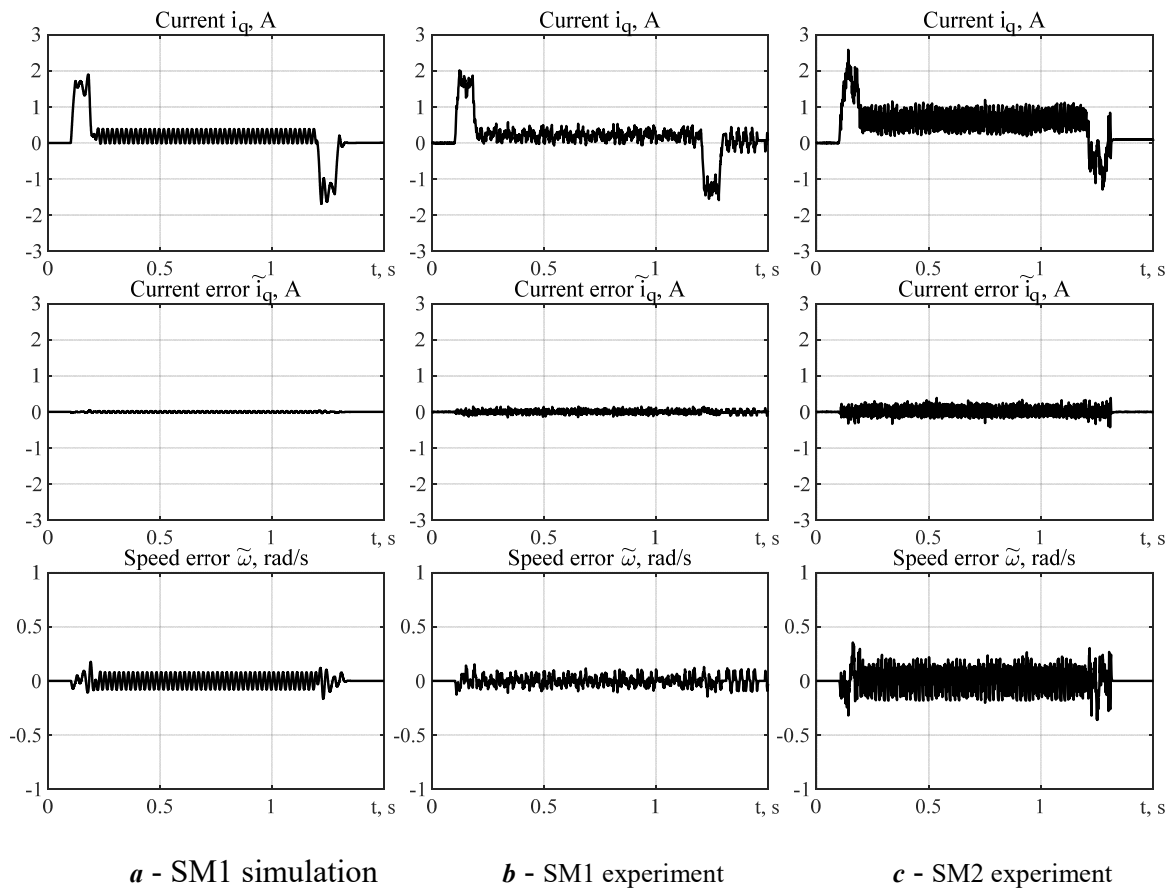
Fig. 5

Simulation transients for SM1 are reported in Fig. 5, a with parasitic torque $T_p = 0.1\sin(2p_n\theta)$ Nm. Quadrature current error is negligibly small ($\tilde{i}_q \approx 0$) that proves the results of error dynamics analysis.

The same test was performed experimentally for both motors. Speed transients are shown in Fig. 5, b, Fig. 5, c for SM1 and SM2, respectively. From speed transients on Fig. 3 and Fig. 5 we conclude: a) torque ripple in SM2 is almost one order higher compared to SM1; b) action of the speed controller suppresses the speed oscillations, caused by torque ripple in SM2, by at least two times.

Position tracking. The operation sequence includes position reference trajectory tracking as shown in Fig. 4, b with maximum values of the derivatives $\dot{\theta}^* = 10$ rad/s $\ddot{\theta}^* = 125$ rad/s^2 and $\dddot{\theta}^* = 6250$ rad/s^3.

Transients of position trajectory tracking are shown in Fig. 6, a and Fig. 6, b for motors SM1 and SM2, respectively. Position and speed controller gains are tuned at $k_\theta = 125$, $k_\omega = 150$, $k_{\omega i} = k_\omega^2 / 2$; current controllers gains remains the same as in the previous test.

a - SM1 experiment   *b* - SM2 experiment
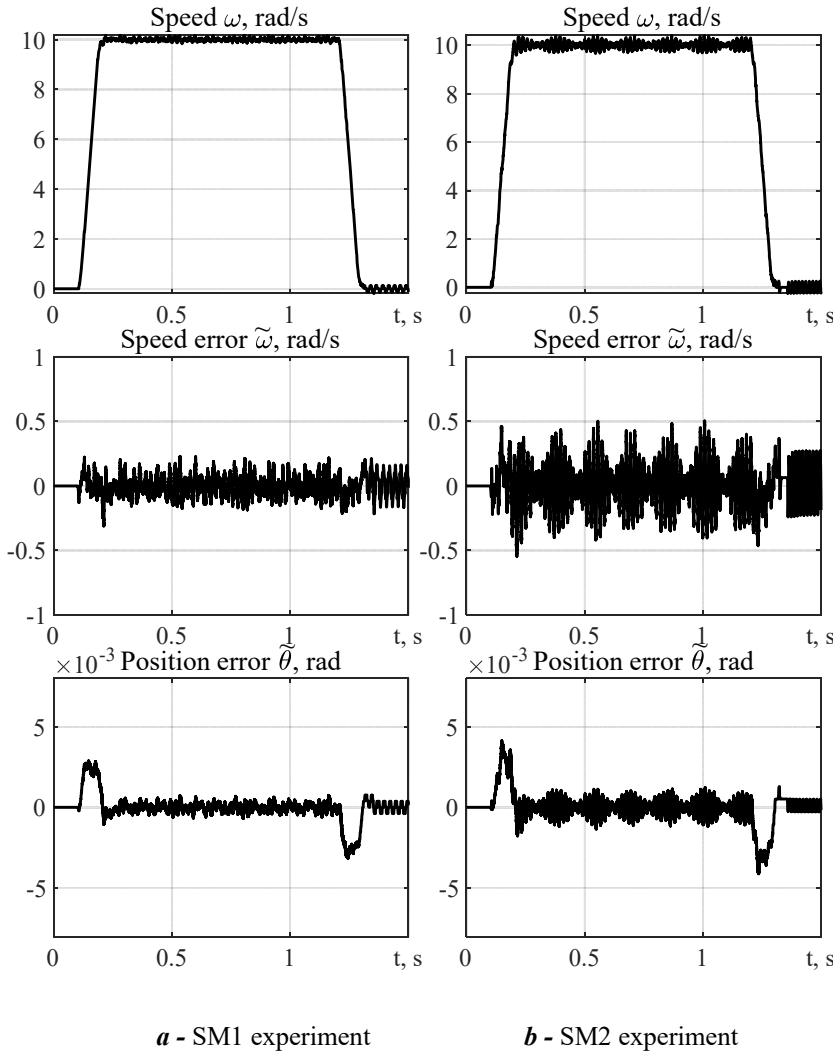
Fig. 6

Precision of the position trajectory tracking is the same for both motors. Position tracking error in steady-state (when $\dot{\theta}^* = \text{const}$) is $\pm 0.8 \times 10^{-3}$ rad for SM1, and $\pm 1.2 \times 10^{-3}$ rad for SM2. During acceleration and deceleration dynamic position tracking error is equal $\pm(3-4) \times 10^{-3}$ rad for both motors.

Conclusions. Performance and robustness of the speed and position feedback linearizing control algorithms for low-cost IPMSM-based direct drives are investigated under condition of high motor torque ripple. Control systems were tested using two motors with different level and content of torque pulsations. Theoretical analysis shows that torque pulsations can be compensated by position and speed feedback controllers, if time scale separation between current and speed control loops is ensured. Position control loop has to be fast enough to compensate for the external disturbances from speed regulation loop. Experimental results prove the results of theoretical findings, since both motors show similar position control performance. Proposed control algorithms can be used for high dynamic applications, as well as in low-cost electric drives with medium performance requirements.

Appendix A. <u>Rated parameters of SM1 ZLLG80ASM250</u>: power P_N = 0.35 kW, current I_N = 8 A, torque T_N = 8 Nm, speed ω_N = 21 rad/s, DC-link voltage 24-48 V, pole pairs p_n = 15, stator resistance R = 0.35 Ohm, d-q inductances L_d = 0.7 mH, L_q = 0.9 mH, permanent magnets flux ψ_m = 0.028 Wb, total inertia J = 0.0073 kgm^2, viscous friction coefficient ν = 0.012 Nm(rad/s)$^{-1}$.

<u>Rated parameters of SM2</u>: power P_N = 0.3 kW, current I_N = 10 A, torque T_N = 8 Nm, speed ω_N = 10 rad/s, DC-link voltage 12 V, pole pairs p_n = 16, stator resistance R = 0.22 Ohm, d-q inductances L_d = 0.3 mH, L_q = 0.6 mH, permanent magnets flux ψ_m = 0.02 Wb, total inertia J = 0.005 kgm^2, viscous friction coefficient ν = 0.012 Nm(rad/s)$^{-1}$.

Appendix B. Algorithm for electrical parameters estimation is presented in [13]. Algorithm guarantees asymptotic identification of resistance R, d-q inductances L_d, L_q and permanent magnet flux ψ_m.

The following current references and tuning gains were used in the test.

SM1: d-q axes current references are $i_d^* = 1\sin(2\pi 5t)$ A, $i_q^* = 2\sin(2\pi 4t)$ A. Tuning gains are $\lambda_1 = 10$, $\lambda_2 = \lambda_3 = 0.0005$, $\lambda_4 = 0.01$, $k_{id} = k_{iq} = 2$. SM2: d-q axes current references are $i_d^* = 1\sin(2\pi 3t)$ A, $i_q^* = 1.8\sin(2\pi 5t)$ A. Tuning gains are $\lambda_1 = 10$, $\lambda_2 = \lambda_3 = 0.0005$, $\lambda_4 = 0.01$, $k_{id} = k_{iq} = 1$. Initial conditions are zero for all parameters.

Estimation process of the parameters for SM1 and SM2 are shown in Fig. 7. After transients, the estimates of the unknown parameters converge to certain steady-state values. As a result, estimated values of the electrical parameters for SM1 are following: stator resistance R = 0.38 Ohm, d-q inductances

$L_d = 0.7$ mH, $L_q = 0.9$ mH, permanent magnets flux $\psi_m = 0.028$ Wb; and for SM2: stator resistance $R = 0.22$ Ohm, d-q inductances $L_d = 0.3$ mH, $L_q = 0.6$ mH, permanent magnets flux $\psi_m = 0.02$ Wb.
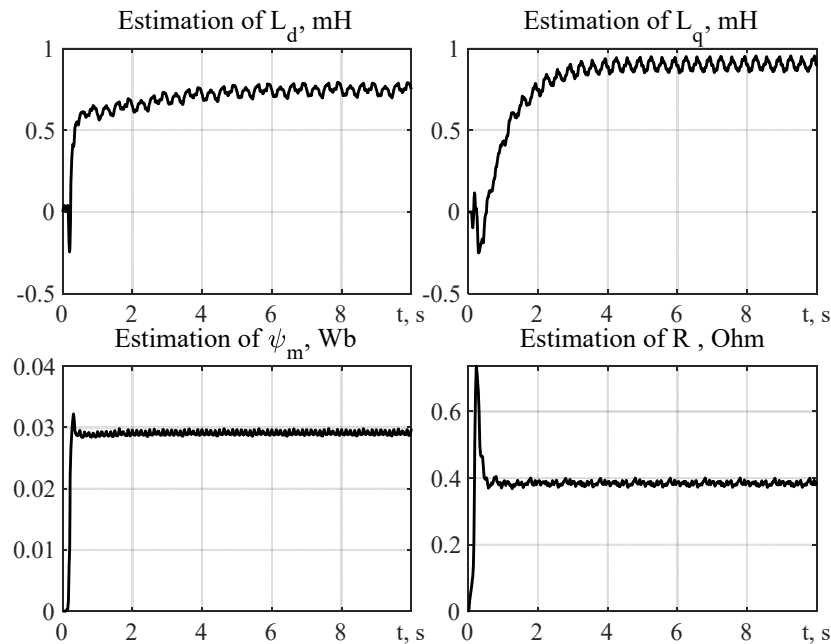
a - SM1 parameters estimation
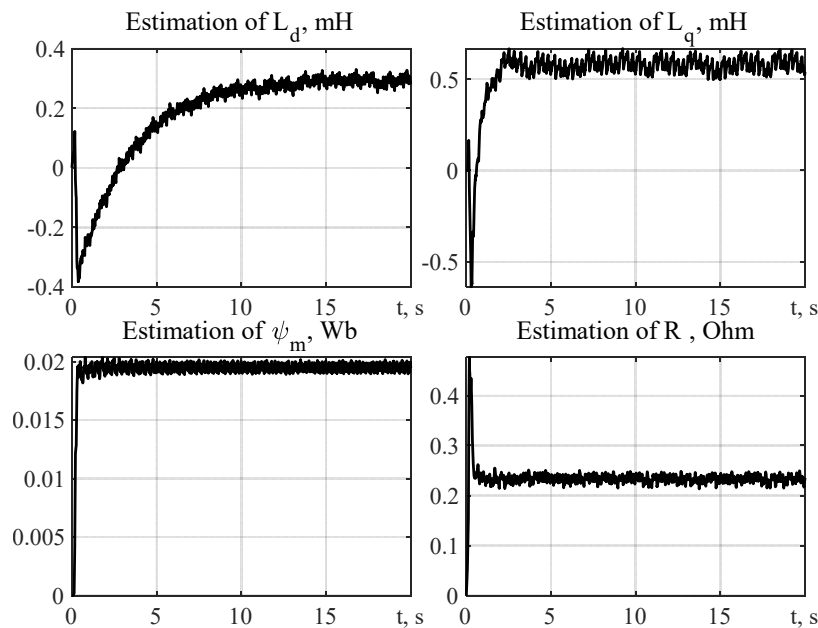
b - SM2 parameters estimation
Fig. 7

1. Holtz J., Springob L. Identification and compensation of torque ripple in high-precision permanent magnet motor drives. *IEEE Transactions on Industrial Electronics*. April 1996. Vol. 43. No 2. Pp. 309-320. DOI: https://doi.org/10.1109/41.491355 .
2. Bianchi N., Bolognani S. Design techniques for reducing the cogging torque in surface-mounted PM motors. *IEEE Transactions on Industry Applications.* Sept.-Oct 2002. Vol. 38. No 5. Pp. 1259-1265. DOI: https://doi.org/10.1109/TIA.2002.802989 .
3. Islam R., Husain I., Fardoun A., McLaughlin K. Permanent-magnet synchronous motor magnet designs with skewing for torque ripple and cogging torque reduction. *IEEE Transactions on Industry Applications*. Jan.-Feb. 2009. Vol. 45. No 1. Pp. 152-160. DOI: https://doi.org/10.1109/TIA.2008.2009653 .

4. Springob L., Holtz J. High-bandwidth current control for torque-ripple compensation in PM synchronous machines. *IEEE Transactions on Industrial Electronics*. Oct. 1998. Vol. 45. No 5. Pp. 713-721. DOI: https://doi.org/10.1109/41.720327.

5. Mattavelli P., Tubiana L., Zigliotto M. Torque-ripple reduction in PM synchronous motor drives using repetitive current control. *IEEE Transactions on Power Electronics*. Nov. 2005. Vol. 20. No 6. Pp. 1423-1431. DOI: https://doi.org/10.1109/TPEL.2005.857559.

6. Jian-Xin X., Panda S.K., Ya-Jun P., Tong H.L., Lam B.H. A modular control scheme for PMSM speed control with pulsating torque minimization. *IEEE Transactions on Industrial Electronics*. June 2004. Vol. 51. No 3. Pp. 526-536. DOI: https://doi.org/10.1109/TIE.2004.825365.

7. Petrovic V., Ortega R., Stankovic A.M., Tadmor G. Design and implementation of an adaptive controller for torque ripple minimization in PM synchronous motors. *IEEE Transactions on Power Electronics*. Sept. 2000. Vol. 15. No 5. Pp. 871-880. DOI: https://doi.org/10.1109/63.867676.

8. Grcar B., Cafuta P., Stumberger G., Stankovic A.M. Control-based reduction of pulsating torque for PMAC machines. *IEEE Transactions on Energy Conversion*. June 2002. Vol. 17. No 2. Pp. 169-175. DOI: https://doi.org/10.1109/TEC.2002.1009464.

9. Weizhe Q., Panda S.K., Jian-Xin X. Torque ripple minimization in PM synchronous motors using iterative learning control. *IEEE Transactions on Power Electronics*. Vol. 19. No 2. Pp. 272-279. March 2004, DOI: https://doi.org/10.1109/TPEL.2003.820537.

10. Zhou Z., Xia C., Yan Y., Wang Z., Shi T. Torque ripple minimization of predictive torque control for pmsm with extended control set. *IEEE Transactions on Industrial Electronics*. September 2017. Vol. 64. No 9. Pp. 6930-6939. DOI: https://doi.org/10.1109/TIE.2017.2686320.

11. Peresada S., Nikonenko Y., Reshetnyk V. Rodkin D. Adaptive position control and self-commissioning of the interior permanent magnet synchronous motors. IEEE International Conference on *Modern Electrical and Energy Systems (MEES)*. Kremenchuk, Ukraine, 23-23 September 2019. Pp. 498-501. DOI: https://doi.org/10.1109/MEES.2019.8896410.

12. Peresada S., Rodkin D., Reshetnyk V. Theoretical and experimental comparison of the standard and feedback linearizing speed controllers for synchronous motors. *IEEE Problems of Automated Electrodrive. Theory and Practice (PAEP)*. Kremenchuk, Ukraine, 21-25 September 2020. Pp. 1-5. DOI: https://doi.org/10.1109/PAEP49887.2020.9240821.

13. Peresada S., Nikonenko Y., Reshetnyk V. Identification of the interior permanent magnet synchronous motor electrical parameters for self-commissioning. IEEE 40th International Conference on *Electronics and Nanotechnology (ELNANO)*. Kyiv, Ukraine, 22-24 April 2020. Pp. 826-831. DOI: https://doi.org/10.1109/ELNANO50318.2020.9088867.

КЕРУВАННЯ ПОЛОЖЕННЯМ НЕДОРОГИХ БЕЗРЕДУКТОРНИХ ПРИВОДІВ НА БАЗІ ЯВНОПОЛЮСНИХ СИНХРОННИХ ДВИГУНІВ З ПОСТІЙНИМИ МАГНІТАМИ

С.М. Пересада, докт. техн. наук, **Д.І. Родькін**, **Є.О. Ніконенко**, **С.М. Ковбаса**, докт. техн. наук, **В.В. Поліщук**
НТУУ «Київський політехнічний інститут ім. Ігоря Сікорського»,
пр. Перемоги, 37, Київ, 03056, Україна,
e-mail: sergei.peresada@gmail.com.

Розглянуто проблему компенсації паразитного моменту для електроприводів на основі недорогих безредукторних явнополюсних синхронних двигунів з постійними магнітами. Властивості робастності систем векторного керування швидкістю і положенням досліджено з використанням принципу розділення у часі контурів регулювання струму, швидкості і положення. Доведено, що динамічна поведінка замкненої системи завдяки новому синтезу алгоритму керування має каскадні властивості з послідовно зв'язаними контурами регулювання швидкості і положення. Таким чином забезпечується можливість компенсації високочастотних паразитних моментів завдяки підвищенню коефіцієнтів налаштування регуляторів. Результати експериментального дослідження на основі двох двигунів з подібними номінальними параметрами, проте з суттєво різним рівнем паразитного моменту свідчать, що незалежно від амплітуди паразитного моменту забезпечується подібна ефективність відпрацювання положення. Запропоновані алгоритми керування можуть бути використаними як для високодинамічних застосувань, так і для недорогих безредукторних електроприводів із середніми вимогами до якості регулювання швидкості і положення. Бібл. 13, рис. 7.

Ключові слова: явнополюсні синхронні двигуни з постійними магнітами, робастне керування швидкістю, керування положенням, паразитний момент.